

# Effects of noisy and modulated interferers on the free-running oscillator spectrum

Sergio Sancho, *Member, IEEE*, Mabel Ponton, *Member, IEEE*, Almudena Suarez, *Fellow, IEEE*

**Abstract**— A new methodology for the prediction of oscillator phase dynamics under the effect of an interference signal is presented. It is based on a semi-analytical formulation in the presence of a noisy or modulated interferer, using a realistic oscillator model extracted from harmonic-balance simulations. The theoretical analysis of the phase process enables the derivation of key mathematical properties, used for an efficient calculation of the interfered-oscillator spectrum. The resulting quasi-periodic spectrum is predicted, as well as the impact of the interferer phase noise and modulation over each spectral component, in particular over the one at the fundamental frequency. It is demonstrated that, under some conditions the phase noise at this component is pulled to that of the interference signal. Resonance effects at multiples of the beat frequency are also predicted. In addition, the effects of interferer phase and amplitude modulation on the oscillator phase dynamics have been studied and compared. For that analysis, efficient simulation techniques have been developed. The analyses have been validated with experimental measurements in a FET-based oscillator at 2.5 GHz, obtaining excellent agreement.

**Index Terms** — Microwave oscillator, frequency-domain analysis, interferer, injection pulling, phase noise, phase modulation, amplitude modulation.

## I. INTRODUCTION

Several are the possible effects of an interferer on the local-oscillator of a communication system. In general, the oscillation frequency will be pulled towards that of the interferer, so a quasi-periodic spectrum is obtained, with the oscillation frequency affected by the interferer [1-3]. Synchronization to the interferer may also occur if the interferer frequency is close enough to the oscillation frequency. Even when the oscillator is inside a phase-locked loop (PLLs), the interferer may pull the voltage-controlled oscillator (VCO) free-running frequency, shifting the whole hold-in range [4]. Besides these frequency-pulling effects, the oscillator phase dynamics can be altered by the interferer noise [5] or modulation.

In this work, the formulation presented in [5] for the study of the interferer influence on the oscillator phase noise has been extended to include the effect of the interferer phase and amplitude modulations on the oscillator phase dynamics. We have limited the investigation to low amplitude interferers, since the strong pulling effects due to a high-power interferer

would disrupt the communication. The study of the impact of the interferer on the phase dynamics of the free-running oscillator is the first stage of our investigation. Even if the frequency pulling effect can be prevented by an afterward phase locking or injection locking of this oscillator, the oscillator phase dynamics can be modified by the interferer. This is because beyond a specific frequency offset from the carrier, the phase-noise spectrum under locked conditions is approximately similar to that of the free-running oscillator [6, 7] (Chapters 2 and 7, respectively). As presented in the manuscript, the analysis may be of practical interest in some systems where the local oscillator operates in free-running conditions, like homodyne FMCW or Doppler radars [8], based on a self-injection-locked oscillator. These systems actually behave in free-running conditions due to the absence of independent sources. Their performance may be preserved when the local oscillator frequency is weakly pulled by an interferer, since the operation principle is based on the frequency difference between two signals (local and returned), generated by the same oscillator. In contrast, the perturbations on the free-running oscillator phase in the form of phase noise or undesired modulation can significantly degrade the circuit behavior [9].

The study focuses on the case in which a low power interferer gives rise to small frequency pulling but degrades the phase-noise spectrum. Predicting the oscillator phase degradation in the presence of an interferer will help correct the prototypes at the design stage, so as to make them more robust against the interferer action. To have an impact on the oscillator spectrum, the interferer frequency must be close to that of the interfered oscillator, as otherwise the two signals will have independent phase variations. The analysis is involved since in the general case of an oscillator that is not locked to the interferer, the solution will be quasi-periodic, with two fundamental frequencies: the oscillation frequency, affected by the interferer, and the interferer frequency [1, 10]. In the previous work [7], a rigorous general formulation for the noise analysis of nonautonomous circuits with multiple inputs is provided. The formulation is derived in terms of the circuit state variables and stochastic analysis techniques are applied to obtain the power spectral density (PSD) of the circuit output variables. This is different from the present work, where emphasis is placed on the autonomous behavior of the interfered oscillator.

Manuscript received July 1, 2017. This paper is an expanded version from the 2017 International Microwave Conference, Honolulu, HI, 4–9 June 2017. This work was supported by the Spanish Ministry of Economy and Competitiveness under the research project TEC2014-60283-C3-1-R, the European Regional Development Fund (ERDF/FEDER) and Juan de la Cierva Research Program IJCI-2014-19141 and by the Parliament of Cantabria under the project

Cantabria Explora 12.JP02.64069.

S. Sancho, A. Suárez and M. Pontón are with the Departamento de Ingeniería de Comunicaciones, Universidad de Cantabria, Santander, 39005, Spain (e-mail: [sanchosm@unican.es](mailto:sanchosm@unican.es); [almudena.suarez@unican.es](mailto:almudena.suarez@unican.es); [mabel.ponton@unican.es](mailto:mabel.ponton@unican.es)).

However, an efficient multirate method is used in [7] to solve separately the variable components corresponding to different time scales. Such a separation will also be necessary in the interferer problem tackled in this work, which considers a circuit with an autonomous frequency component due to the oscillation and a nonautonomous component due to the interferer.

From a harmonic-balance (HB) simulation viewpoint [11], the only way to address the oscillator phase-noise analysis in the presence of an additional noisy fundamental is through a two-stage procedure. The first stage should be a two-tone simulation, with one autonomous fundamental, able to account for the small pulling effects. The second stage should be a phase-noise analysis of the oscillator carrier. However, under a small difference between the interferer and oscillation frequencies, the HB Jacobian matrix is usually ill-conditioned, leading to convergence problems and an inaccurate prediction of the phase-noise spectrum.

On the other hand, in the case of a modulated interferer, in ordinary envelope transient simulations of autonomous circuits, there is usually a shift between the actual oscillation frequency  $f_{osc}$  and the fundamental frequency of the Fourier-series, fixed by the user [12]. This frequency shift introduces a phase ramp that contaminates the spurious modulation effects. To obtain the oscillation signal, the envelope time step must be sufficiently small to account for this frequency shift. In the presence of a narrow-band modulation signal, the relatively small step will give rise to a high computational cost.

Here, in order to circumvent these problems, a semi-analytical method is proposed. This method allows the derivation of a stochastic differential equation for the autonomous phase, which acts as the single state variable of the system. A realistic model of the interfered oscillator is used, based on derivatives obtained through finite differences in HB, calculated about the free-running point [13-15]. The analysis relies on the determination of the phase perturbation of the interfered oscillator in the presence of the undesired signal, as well as its own noise sources. Limit forms of the stochastic analysis in the frequency domain are applied to approach the interferer influence on the far carrier phase noise spectrum. In addition, a multirate method similar to the one in [7] is used to solve numerically the transference of the interferer phase modulation to the oscillation autonomous component.

In Section II, the equation governing the oscillation phase in the presence of a noisy or modulated interferer will be derived. In Section III, a formulation based on this equation will be developed to analyze the effect of the interferer phase noise on the oscillation phase noise characteristic. Finally, in Section IV, the effects of phase and amplitude modulated interferers on the oscillation phase will be studied and compared. The mechanisms producing spurious modulation of the oscillator phase will be explained in detail. All the analytical and simulation results will be compared with measurements in a FET-based oscillator at 2.5 GHz.

## II. GENERAL FORMULATION FOR THE ANALYSIS OF THE INTERFERER INFLUENCE

### A. Derivation of the nonlinear model

The analysis will be illustrated through its application to the

FET-based oscillator at  $f_{osc} = 2.5$  GHz in Fig. 1. In the proposed experiment, an interference signal with carrier frequency  $f_{in}$  enters the output port through a circulator. The interferer is modeled by its Norton equivalent with a current source  $i_g(t)$ . Interference signal entering through the output port is a realistic situation in front-end systems. However, the formulation can be equally applied for other locations of the interference equivalent source. It will be derived in terms of the voltage signal  $v(t)$  at the transistor drain terminal, although, in general, the analysis can be performed for any other node of observation. Note that the analysis can be performed at a node different from the one where the interferer current source is connected, since its effect is modeled by means of transfer functions [13-15].

In this circuit, the white noise sources are the thermal sources associated to resistive elements and the channel noise generated by the DC transconductance, whereas the colored noise source is the flicker source associated to the FET device. Using the technique in [16], the effect of all the white and colored [17, 18] noise sources existing in the circuit has been modeled with an equivalent current generator  $i_n(t)$  connected in parallel at the transistor drain. The PSD of this current source is extracted from HB commercial software simulations of the free-running oscillator. The technique does not require the explicit knowledge of all the noise sources present in the oscillator. It is based on the fitting of a single noise source  $i_n(t)$ , located at the node where the interferer signal enters the circuit. In a circuit-level phase-noise analysis of the non-interfered oscillator, this source is fitted so as to provide the same phase-noise spectrum as the complete set of oscillator noise sources in the resistive elements and active devices.

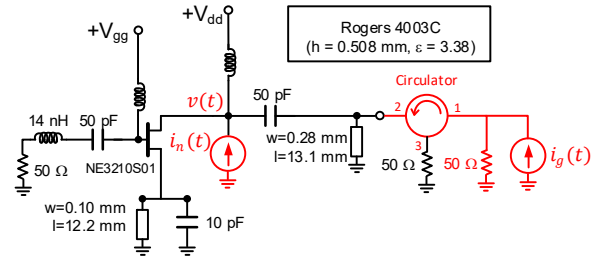


Fig. 1. Schematic of the interfered oscillator operating at  $f_{osc} = 2.5$  GHz based on the FET NE3210S01. The interference is modeled with a current source and introduced into the oscillator through a circulator

The interferer and noise equivalent sources will be expressed as:

$$\begin{aligned} i_g(t) &= 2\text{Re}\{U(t)e^{j\omega_{in}t}\}, \quad U(t) = I_g(t)e^{j[\psi(t)+\theta_g]} \\ i_n(t) &= 2\text{Re}\{I_n(t)e^{j\omega_{in}t}\} \end{aligned} \quad (1)$$

with  $\omega_{in} = 2\pi f_{in}$  and the amplitude and phase components  $I_g(t) \in \mathbb{R}$  and  $\psi(t) \in \mathbb{R}$  accounting in general for modulation or noise processes. The noise current source  $i_n(t)$  has been modeled by means of a single time-varying harmonic component  $I_n(t)$ . The introduction of the source  $i_g(t)$  perturbs each  $q$ -th harmonic component of the signal  $v(t)$ :

$$v(t) = \sum_{q=-Q}^Q v_q(t), \quad v_q(t) = X_q(t)e^{jq\omega_{in}t}, \quad (2)$$

$$X_q(t) = [V_q + \Delta V_q(t)]e^{j\theta_q(t)}$$

where each  $v_q(t)$  is a narrow band process centered at the frequency component  $qf_{in}$ . While the interferer produces small amplitude perturbation components  $\Delta V_q(t)$ , the phase components  $\theta_q(t)$  are unbounded in the non-synchronized state [1]. Now, following the semi-analytical formulation technique (SAF) proposed in [13-15], the Kirchhoff current law is applied to the observation node focusing on the equation corresponding to the first harmonic component. Then, the Implicit Function Theorem is applied to obtain an envelope-domain model of the oscillator dynamics in the form of a single outer-tier equation:

$$Y[V_1 + \Delta V_1(t), j(\omega_{osc} + \Delta\omega) + s, U^r(t), U^i(t)] = \frac{I_n(t)e^{-j\phi(t)}}{V_1 + \Delta V_1(t)} \quad (3)$$

where  $Y$  is the first harmonic total admittance at the observation node, and  $\Delta\omega = 2\pi\Delta f = \omega_{osc} - \omega_{in}$ , with  $\omega_{osc} = 2\pi f_{osc}$  being the free-running frequency. The super-indexes  $r, i$  mean real and imaginary parts of the corresponding signals. The phase  $\phi(t) \equiv \theta_1(t)$  represents the first-harmonic phase component at the interferer frequency  $f_{in}$ . In this work, an interference phenomenon perturbing the steady state oscillation up to the first order will be considered. This case is quite realistic, since the interferer usually enters the oscillator core after crossing filtering paths or electromagnetic shields, which makes its influence on equation (3) small. Then, equation (3) can be approximated by a first-order Taylor series about the free-running state. Following a similar procedure as in previous work [15], this approximation yields the following equation for the phase shift:

$$\dot{\phi} = \Delta\omega + K_s(t)\sin[\phi - \psi(t)] + K_c(t)\cos[\phi - \psi(t)] + \varepsilon(t) \quad (4)$$

$$\varepsilon(t) = H^r I_n^r(t) + H^i I_n^i(t)$$

with:

$$K_s(t) = \frac{B_s(t) \cdot Y_V}{Y_\omega \times Y_V}, \quad K_c(t) = \frac{B_c(t) \times Y_V}{Y_\omega \times Y_V}, \quad (5)$$

$$H = \frac{1}{V_1} \frac{Y_V^i - jY_V^r}{Y_\omega \times Y_V}$$

where the simplifying relations  $a \cdot b = a^r b^r + a^i b^i$  and  $a \times b = a^r b^i - a^i b^r$  have been introduced. The coefficients  $K_c(t), K_s(t), H^r, H^i$  are provided in terms of the derivatives of the admittance function (3) evaluated at the free-running solution:

$$Y_V = \frac{\partial Y(V_1, \omega_o, 0, 0)}{\partial V}, \quad Y_\omega = \frac{\partial Y(V_1, \omega_o, 0, 0)}{\partial \omega} \quad (6)$$

$$B_s(t) = j \frac{I_g(t)}{V_1} Y_{U^r}, \quad B_c(t) = -\frac{I_g(t)}{V_1} Y_{U^i},$$

$$Y_{U^{r,i}} = \frac{\partial Y(V_1, \omega_o, 0, 0)}{\partial U^{r,i}}$$

According to equation (4), a constant shift of the interferer phase  $\psi(t)$  will produce a shift of the same amount in the phase  $\phi(t)$ , which will not affect the spectrum of  $v_1(t)$ . Then, without loss of generality, in the following  $\theta_g = 0$  will be assumed to simplify the formulation. Note that, as a difference from [15], the coefficients  $K_c(t), K_s(t)$  are time dependent to model the effect of the interferer amplitude modulation  $I_g(t)$ . The admittance derivatives  $Y_V, Y_\omega, Y_{U^{r,i}}$  in (6) can be calculated through finite differences in commercial HB following the technique described in [15]. Equation (4) provided by the SAF technique can be used to calculate the oscillator phase dynamics in the presence of a noisy and modulated interferer.

### B. Validity of the proposed model

The first-order model is composed of the derivatives of the oscillator total-admittance function, calculated with respect to the node amplitude, frequency and interference signal, evaluated at the (non-interfered) free-running point. All the rest of circuit variables and harmonic frequencies are taken into account when applying finite differences to the auxiliary generator [13-15] used for the practical calculation of these derivatives. The modeling procedure is totally general and independent of the particular oscillator circuit and its operation frequency. However, there is a limitation on the interferer power, which should be sufficiently small for the first-order Taylor-series expansion to be applicable. In fact, the analysis presented is most relevant for a low interferer power. For too high power, frequency-pulling effects would be so strong that the oscillator would significantly impair the communication system.

To evaluate the validity of the proposed approach, the oscillator is assumed to be injection-locked by the interference of a particular amplitude  $I_g$ , even though this regime is not the object of this investigation. The synchronization bandwidth is calculated both through the semi-analytical method, based on the first-order Taylor series approximation, and using a circuit-level harmonic-balance simulation, with the aid of one auxiliary generator [13-15]. The two analyses are computationally undemanding. If the synchronization bands agree with the two different methods, the first-order approximation must be a valid one, so it will be applicable in unlocked conditions for the interferer amplitude  $I_g$ . The accuracy evaluation under injection-locked conditions takes advantage of the oscillator operation in a periodic regime, much simpler to analyze than the unlocked quasi-periodic one that is the object of this investigation.

Let us consider the case of a noise and modulation-free interferer of amplitude and phase  $I_g, \psi$ . As stated in [1], the oscillation can synchronize to the interferer provided the frequency difference  $|\Delta f| = |f_{osc} - f_{in}|$  is below a bifurcation limit, with  $f_{osc}$  being the oscillation frequency in the absence of the interferer. In the synchronized state, the frequency difference  $\dot{\phi}(t)$  between the oscillation and the interferer vanishes. In that case, model (4) predicts the set of interferer frequency values providing synchronized solutions:

$$f_{in} = f_{osc} + \frac{1}{2\pi}(K_s \sin \alpha + K_c \cos \alpha), \quad \alpha \in [0, 2\pi] \quad (7)$$

with  $\alpha = \phi - \psi$ . This prediction can be validated by comparison with the synchronization range using a circuit-level HB simulation, with the aid of an auxiliary generator [19, 20]. The two analyses are computationally undemanding. If the synchronization bands agree with the two different methods, the first-order approximation must be a valid one, so it will be applicable in unlocked conditions for the interferer amplitude  $I_g$ .

As an example, this comparison has been carried out in Fig. 2 for two values of the interferer amplitude. In the first case, for  $I_g = 0.3$  mA the synchronization range predicted with equation (7) agrees with the one obtained in commercial HB software. This indicates that model (4) is valid for this interferer amplitude. In the second case, for  $I_g = 1.4$  mA, the disagreement between the results of equation (7) and the commercial HB software indicates that the interferer amplitude is too high for model (4) to be accurate.

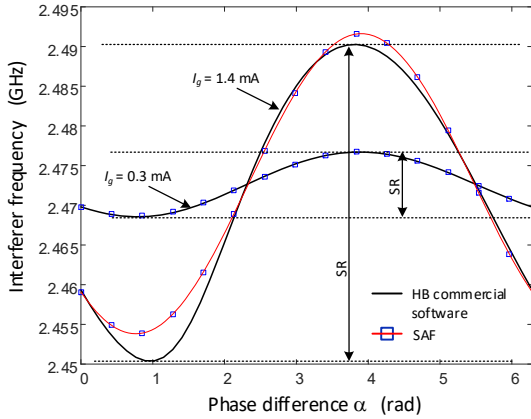


Fig. 2. Synchronization range (SR). Comparison between SAF model (7) and simulation in commercial HB software.

In this paper, the non-synchronized case, i.e. the case of an interferer with frequency  $f_{in}$  out from the synchronization range, will be analyzed. Note that once model (4) is validated for a given value of the interferer amplitude, the interferer influence will decrease and eventually become negligible as the frequency difference  $|\Delta f| = |f_{osc} - f_{in}|$  grows. The narrow-band noisy or modulated interferer considered in the subsequent Sections will introduce small amplitude or frequency perturbations, with negligible influence on the model validity.

### III. PHASE NOISE ANALYSIS

The phase noise is given by the perturbation component of the phase variable  $\phi(t)$  due to the effect of the noise sources present in  $i_n(t)$  and  $i_g(t)$ . In the absence of the interferer, equation (4) gets simplified and the noise current source  $i_n(t)$  produces the same phase noise spectrum as the HB commercial software applied to the free-running oscillator. In order to calculate the phase noise of the interfered oscillator, in the first place the steady-state solution in the absence of interferer modulation and noise sources must be analyzed.

#### A. Phase dynamics in the absence of interferer modulation and noise sources

In this case, equation (4) represents an autonomous system that can be written as:

$$\dot{\phi} = \Delta\omega + K_s \sin \phi + K_c \cos \phi = g(\phi) \quad (8)$$

with  $K_c, K_s$  being constant coefficients. The phase shift becomes a constant value  $\phi = \phi_s$ , fulfilling  $g(\phi_s) = 0$ , only when the free-running frequency synchronizes to the interferer. Then, in the more general unsynchronized conditions  $g(\phi) \neq 0$ ,  $\forall \phi$  must be fulfilled, implying that  $\phi(t)$  grows or decreases monotonically. This fact, together with the system autonomy, produces an accumulation effect of the numerical error associated to the time integration resolution of equation (8). As it will be explained in Section III.B, this error may produce qualitative changes on the predicted spectrum about the free-running frequency in the presence of the interferer. To overcome this problem, the following procedure is followed. Let us assume that  $g(\phi) > 0$ ,  $\forall \phi$ . The case  $g(\phi) < 0$ ,  $\forall \phi$  is symmetric. The time required by the phase variable to pass through an arbitrary interval  $[\phi_a, \phi_b]$  is given by:

$$\begin{aligned} T(\phi_a, \phi_b) &= \int_{\phi_a}^{\phi_b} \frac{d\phi}{g(\phi)} = \\ &= u_0(\phi_b - \phi_a) + q(\phi_b) - q(\phi_a), \\ u(\phi) &= \frac{1}{g(\phi)} = u_0 + \tilde{u}(\phi), \quad u_0 = \frac{1}{2\pi} \int_0^{2\pi} u(\phi) d\phi, \\ q(\phi) &\equiv \int \tilde{u}(\phi) d\phi, \quad q(\phi) = q(\phi \pm 2\pi) \end{aligned} \quad (9)$$

Note that the  $\phi$ -periodic function  $u(\phi)$  has been separated into its dc component  $u_0$  and the term  $\tilde{u}(\phi)$  fulfilling

$$\int_0^{2\pi} \tilde{u}(\phi) d\phi = 0 \quad (10)$$

From the definition of  $g(\phi)$ , the phase shift fulfills:

$$\begin{aligned} T_b = T(\phi, \phi + 2\pi) &= u_0 2\pi + q(\phi + 2\pi) - q(\phi) = \\ &= u_0 2\pi, \quad \forall \phi \end{aligned} \quad (11)$$

Property (11) implies that  $\dot{\phi}(t)$  is periodic, since:

$$\begin{aligned} \dot{\phi}(t + T_b) &= g[\phi(t + T_b)] = g[\phi(t) + 2\pi] \\ &= g[\phi(t)] = \dot{\phi}(t) \end{aligned} \quad (12)$$

Considering (11)-(12), the phase variable can be expressed as:

$$\phi(t) = \omega_b t + \sum_{n=-N}^N P_n e^{jn\omega_b t}, \quad \omega_b = 2\pi f_b = 2\pi/T_b \quad (13)$$

The components  $\{f_b, P_{-N}, \dots, P_N\}$  can be calculated in the frequency domain by introducing expression (13) in equation (8) and solving the resulting HB system:

$$\omega_b + jn\omega_b P_n = G_n(\bar{P}, \omega_b), \quad n = -N, \dots, N \quad (14)$$

where  $\bar{P}$  is the vector containing the harmonic components  $P_n$

and each  $G_n$  is the  $n$ -th harmonic component of the  $T_b$ -periodic signal  $g[\phi(t)]$ . System (14) contains  $2N + 1$  equations and  $2N + 2$  unknowns  $\{f_b, \bar{P}\}$ . It can be balanced by making use of the autonomy of equation (8). Due to this autonomy, solution (13) fulfills (8) for any arbitrary constant time shift  $\tau$  of the form:

$$\begin{aligned} \phi(t + \tau) &= \omega_b(t + \tau) + \sum_{n=-N}^N P_n e^{jn\omega_b(t+\tau)} = \\ &= \omega_b t + \sum_{n=-N}^N P_n(\tau) e^{jn\omega_b t}, \quad P_n(\tau) = \begin{cases} P_n e^{jn\omega_b \tau}, & n \neq 0 \\ P_0 + \omega_b \tau, & n = 0 \end{cases} \end{aligned} \quad (15)$$

Then, we can select  $\tau$  to fix  $P_1^i(\tau) = 0$ , where the superindex  $i$  means imaginary part. This additional equation is combined with system (14) to balance the number of equations and unknowns, yielding an algebraic system solvable by a number of optimization techniques, like Newton-Raphson. Once the unknowns  $\{f_b, \bar{P}\}$  are calculated, expression (13) is used to obtain the process  $v_1(t)$  in (2), providing the spectrum nearby the interference frequency  $f_{in}$ . The envelope of this process is  $X_1(t)$ , which can be expanded in Fourier series as:

$$\begin{aligned} X_1(t) &\approx V_1 e^{j\phi(t)} = V_1 e^{j\omega_b t} \exp \left\{ \sum_{n=-N}^N jP_n e^{jn\omega_b t} \right\} = \\ &= \sum_{k=-M}^M X_1^k e^{jk\omega_b t} \end{aligned} \quad (16)$$

where expression (13) has been applied. Then, the spectrum of  $v_1(t)$  has the form:

$$\begin{aligned} v_1(t) &= X_1(t) e^{j\omega_{in} t} = \sum_{k=-M}^M X_1^k e^{j\omega_k t}, \\ \omega_k &= 2\pi f_k = 2\pi(f_{in} + kf_b) \end{aligned} \quad (17)$$

Equation (17) implies that  $v_1(t)$  is a multi-tone signal containing the components  $X_1^k$  at the intermodulation frequencies  $f_k = f_{in} + kf_b$ . For this reason,  $f_b$  will be called the *beat frequency*. The oscillator free-running frequency is pulled from  $f_{osc}$  to  $f'_{osc} \equiv f_1 = f_{in} + f_b$ . This theoretical result has been verified for the case of an interferer with amplitude  $I_g = 0.2$  mA and frequency  $f_{in} = f_{osc} + 10$  MHz. In the first place, the unknowns  $\{f_b, \bar{P}\}$  have been calculated by solving system (14) with  $N = 5$  harmonics, together with the additional equation  $P_1^i = 0$ . Then, the phase shift  $\phi(t)$  has been properly sampled and introduced in the function  $X_1(t) \approx V_1 e^{j\phi(t)}$  to obtain  $M = 10$  coefficients  $X_1^k$  of the Fourier series (16) at the frequencies  $kf_b$ .

The spectrum in Fig. 3 contains the frequency components of the interfered oscillator spectrum at  $f_k = f_{in} + kf_b$ , with  $f_{in}$  and  $f_b$  being the interferer and beat frequencies, respectively. In the SAF the value of the beat frequency  $f_b$  is calculated through numerical resolution of system (14). For comparison, the spectrum of the time-varying first harmonic component  $X_1(t)$  has been obtained in HB commercial software using the envelope transient technique [21-23]. The beat frequency  $f_b$

calculated through both techniques may differ slightly due to fact that the envelope-transient method takes into account the interferer effect at all the harmonic terms  $qf_{in}$  with  $-Q \leq q \leq Q$ , and the SAF only takes into account the interferer effect at the fundamental frequency  $f_{in}$ . This discrepancy becomes more evident for the high-order components  $f_k = f_{in} + kf_b$ , as  $k$  gets increased. In this figure, the harmonic components  $X_1^0$  and  $X_1^1$  corresponding respectively to the interferer and the free-running component are indicated. Observe that the free-running frequency has been pulled from its unperturbed value  $f_{osc} = f_{in} - 10$  MHz to  $f'_{osc} \equiv f_1 = f_{in} + f_b$ , with  $f_b \approx -8$  MHz. Note that the frequency pulling phenomenon can be observed even in the presence of a small amplitude interferer, provided that the frequency difference  $|f_{in} - f_{osc}|$  is small enough, as demonstrated in [1].

The frequency domain technique (13)-(14) represents a significant advance from previous work [14], where equation (8) was solved through a time integration technique. Apart from avoiding the already mentioned accumulation of numerical error, the new method is less computationally costly due to the small number of unknowns  $\{f_b, \bar{P}\}$  to be calculated.

Note that in the case of a phase-locked loop (PLL) or an injection-locked oscillator the situation would be different. In those cases, the admittance function  $Y$  in (3) has a dependence on the amplitude and phase components of the reference or external generator signal [16, 24]. This dependence removes the system autonomy of the interfered system quasi-periodic solution. Therefore, the interfered system does not remain invariant under phase shifts, providing different phase noise results than the autonomous case, which will be the one analyzed here.

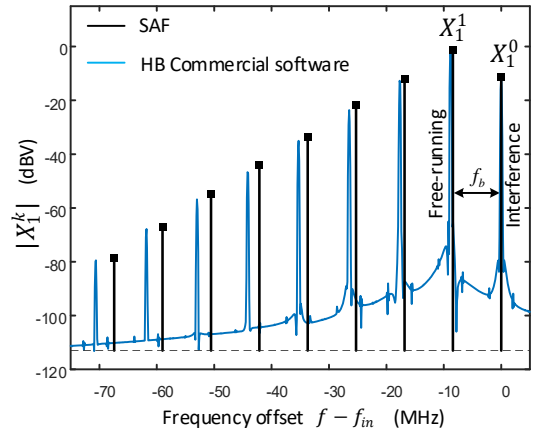


Fig. 3. Spectrum of the first harmonic component  $X_1(t)$  of the drain voltage  $v(t)$  in the presence of an interferer with  $I_g = 0.2$  mA and  $\Delta f = -10$  MHz.

### B. Phase perturbation due to the noise sources

Let  $\phi(t) = \phi_0(t)$  be the phase shift in absence of noise sources. The interferer phase noise will be modeled by the input source time-varying phase  $\psi(t)$ , considered as a small amplitude stochastic process, whereas its amplitude  $I_g$  remains constant. The noisy components introduced by the local sources and the interferer perturb the steady state  $\phi_0(t)$  in the form  $\phi(t) = \phi_0(t) + \Delta\phi(t)$ . Provided  $\Delta\phi(t)$  is small, equation (4) can be linearized about  $\phi_0(t)$  obtaining:

$$\begin{aligned}\Delta\phi(t) &= b_0(t)[\Delta\phi(t) - \psi(t)] + \varepsilon(t), \\ b_0(t) &\equiv \frac{dg[\phi_0(t)]}{d\phi} = K_s \sin \phi_0(t) + K_c \cos \phi_0(t)\end{aligned}\quad (18)$$

Equation (18) shows that the phase perturbation is governed by a linear time-variant (LTV) stochastic differential equation determined by the  $T_b$ -periodic function  $b_0(t)$  and the noise sources  $\varepsilon(t)$  and  $\psi(t)$ . Here, this equation will be solved by means of a time-frequency formulation, expressing the variables in a Fourier series with fundamental frequency  $f_b$ , in terms of time-varying harmonic components. Following this procedure, the term of local noise sources  $\varepsilon(t)$  is expressed as [25]:

$$\begin{aligned}\varepsilon(t) &= \varepsilon_w(t) + \varepsilon_c(t), \quad \langle \varepsilon_w(t_1)\varepsilon_w(t_2)^* \rangle = \Gamma\delta(t_1 - t_2), \\ \varepsilon_w(t) &= \sum_{n=-N}^N E_n(t)e^{jn\omega_b t}, \\ E_n(t) &= \int_{-B/2}^{B/2} E_n(f)e^{j2\pi f t} df, \quad \langle E_k(f)E_l^*(f) \rangle = \frac{\Gamma}{2N}\delta_k^l\end{aligned}\quad (19)$$

where  $\delta_k^l$  is the Kronecker delta,  $\varepsilon_w(t)$  and  $\varepsilon_c(t)$  represent respectively the contributions of the local white and colored noise sources, and  $E_n(t)$ ,  $\psi(t)$  and  $\varepsilon_c(t)$  are uncorrelated base-band stochastic processes with bandwidth  $B$ . The structure of the PSD function  $\langle |\varepsilon_c(f)|^2 \rangle$  depends on the type of colored sources present in the circuit. Due to the structure of the noise sources, the phase perturbation is a cyclo-stationary process that can be expressed as:

$$\begin{aligned}\Delta\phi(t) &= \sum_{n=-N}^N \Theta_n(t)e^{jn\omega_b t}, \\ \Theta_n(t) &= \int_{-B/2}^{B/2} \Theta_n(f)e^{j2\pi f t} df\end{aligned}\quad (20)$$

where each time-varying harmonic  $\Theta_n(t)$  is a base-band process with bandwidth  $B$ . Introducing expression (20) in equation (18) and equating the terms that correspond to the same harmonic order the following linear time-invariant (LTI) system of stochastic differential equations is obtained:

$$\begin{aligned}jn\omega_b \Theta_n(t) + \dot{\Theta}_n(t) &= \sum_{l=-N}^N B_{n-l}\Theta_l(t) - B_n\psi(t) + \\ &+ E_n(t) + \delta_n^0 \varepsilon_c(t), \quad n = -N, \dots, N\end{aligned}\quad (21)$$

with each  $B_n$  being the harmonic component of  $b_0(t)$  at the frequency  $nf_b$ . These harmonics can be numerically obtained through equation (18) from the components  $\{f_b, \bar{P}\}$ . The noisy process  $v_1(t)$  is obtained by introducing expression (20) in expansion (16):

$$\begin{aligned}X_1(t) &= \exp\left\{\sum_{n=-N}^N \Theta_n(t)e^{jn\omega_b t}\right\} \sum_{k=-M}^M X_1^k e^{jk\omega_b t} = \\ &= \exp\left\{\sum_{n \neq 0} \Theta_n(t)e^{jn\omega_b t}\right\} \sum_{k=-M}^M X_1^k e^{j[k\omega_b t + \Theta_0(t)]} \approx \\ &\approx \sum_{k=-M}^M X_1^k(t)e^{jk\omega_b t}, \quad X_1^k(t) = X_1^k e^{j\Theta_0(t)}\end{aligned}\quad (22)$$

where high order terms in the perturbation harmonics  $\Theta_n(t)$  have been neglected. Equation (22) shows that the harmonic components  $X_1^k(t)$  become time varying due to the effect of the noise sources. In particular, the phase noise about  $f'_{osc} \equiv f_1$  is given by the PSD  $S_1(f)$  of the normalized process  $X_1^1(t)/|X_1^1| = e^{j\Theta_0(t)}$  [7, 18, 25-27]. As stated in [18, 26, 28], far enough from the carrier, the PSD  $S_1(f)$  can be approached by the second order moment  $\langle |\Theta_0(f)|^2 \rangle$ . This moment is obtained by translating system (21) to the frequency domain. Assuming small interferer amplitude, harmonic components  $B_n$  with  $|n| > 1$  are neglected, obtaining the system:

$$\begin{aligned}j2\pi(-f_b + f)\Theta_{-1}(f) &= B_{-1}\Theta_0(f) - B_{-1}\psi(f) + E_{-1}(f), \\ j2\pi f\Theta_0(f) &= B_{-1}\Theta_1(f) + B_0\Theta_0(f) + B_1\Theta_{-1}(f) + \\ &+ \varepsilon_c(f) + E_0(f) - B_0\psi(f), \\ j2\pi(f_b + f)\Theta_1(f) &= B_1\Theta_0(f) - B_1\psi(f) + E_1(f)\end{aligned}\quad (23)$$

The second equation of system (23) shows that the direct conversion between the interferer phase noise  $\psi(t)$  and  $\Theta_0(t)$  is due to the harmonic component  $B_0$ . In unsynchronized conditions, this component can be calculated as:

$$\begin{aligned}B_0 &= \frac{1}{T_b} \int_0^{T_b} b_0(t) dt = \frac{1}{T_b} \int_0^{T_b} \frac{dg[\phi_0(t)]}{d\phi} dt = \\ &= \frac{1}{T_b} \int_{g(0)}^{g(T_b)} \frac{dg}{g} = \frac{1}{T_b} \log \frac{g(T_b)}{g(0)} = \frac{1}{T_b} \log \frac{\phi_0(T_b)}{\phi_0(0)} = 0\end{aligned}\quad (24)$$

where  $g = \dot{\phi}_0$  has been applied. Consequently, there is no direct conversion from the interferer phase noise  $\psi(t)$  to  $\Theta_0(t)$ . This is a key result that is in contrast with the synchronized case, where  $\phi_0$  becomes constant and  $b_0(t)$  in (18) agrees with its dc value  $B_0$ . The application of the property  $B_0 = 0$  to system (23) allows, after some algebra, the extraction of the following intuitive equation that models the phase noise at the pulled free-running frequency in the presence of the interferer:

$$\langle |\Theta_0(f)|^2 \rangle \approx \left[ \frac{\alpha}{\alpha + 4\pi^2(f^2 - f_b^2)} \right]^2 \langle |\psi(f)|^2 \rangle + \frac{\langle |\varepsilon(f)|^2 \rangle}{4\pi^2 f^2} \quad (25)$$

where  $\alpha = 2|B_1|^2$  acts as a sensitivity coefficient that determines the influence of the interferer phase noise,  $f$  is the frequency offset from the carrier at  $f_1 = f'_{osc}$  and the second term is the oscillator's own phase noise. Equation (25) is valid for large enough values of the frequency offset  $f$ . In order to obtain equation (25) small interferer amplitude has been assumed. In other cases, system (21) should be translated to the frequency domain considering a higher number  $N$  of harmonic coefficients  $B_n$ . In the absence of an interferer  $\alpha$  becomes zero

and equation (25) agrees with the free-running oscillator phase noise. The introduction of the interferer provides  $\alpha > 0$ , increasing the level of the phase noise characteristic, since it adds a term proportional to the interferer phase noise. The interferer influence is most noticeable when its phase noise characteristic is higher than that of the free-running oscillator. In that case, equation (25) predicts that the phase noise characteristic about  $f'_{osc}$  is pulled towards the interferer phase noise curve. This behavior has been verified in Fig. 4, where the measured phase noise spectrum and the one predicted by equation (25) (SAF) have been compared. In the measurement, the Direct Spectrum Technique has been applied, using the phase noise measurement personality in an Agilent PSA Spectrum Analyzer E4446A (option 226). The resolution bandwidth and video bandwidth of the measured spectra is RBW = 10 kHz and VBW = 10 kHz (respectively). For the analysis, an interferer with  $P_{in} = -29$  dBm and  $f_{in} = f_{osc} + 3$  MHz has been introduced. Due to the pulling effect, the oscillation frequency is shifted to  $f'_{osc} = f_{in} - f_b$ , with  $f_b \approx 2$  MHz. The interferer is not represented. Instead, its measured phase noise from zero offset frequency is traced for comparison. As predicted by (25), the oscillator phase noise is pulled to that of the interferer. Equation (25) also demonstrates a resonance effect, with maximum phase noise at an offset frequency about  $f_b$ . Note that the singularity predicted by (25) at  $f_b$  is fully consistent with the presence of a steady-state spectral line at  $f_2 = f'_{osc} + f_b$ . In the measurement, several resonances at frequency offsets  $kf_b$  for  $k > 1$  are observed, corresponding to the intermodulation components  $X_1^k$  of the interfered spectrum predicted in Section III.A. In order to obtain an intuitive result, in the derivation of equation (25) only the terms  $B_k$  up to  $k = 1$  have been considered. Therefore, only the first resonance at  $f_b$  can be predicted. The rest of resonances could be obtained by considering the corresponding coefficients  $B_k$  for  $k > 1$  when translating system (21) to the frequency domain.

Note that the key property (24) has enabled the prediction of a phase noise spectrum which is qualitatively different to that of the synchronized case, where the phase noise characteristic agrees with that of the interferer up to a frequency offset from the carrier [5]. The result  $B_0 \approx 0$  is numerically obtained when using  $\phi_0(t)$  calculated from the frequency domain technique (13)-(14), while this result is often unobserved when solving equation (8) through time integration, due to the cumulative numerical error.

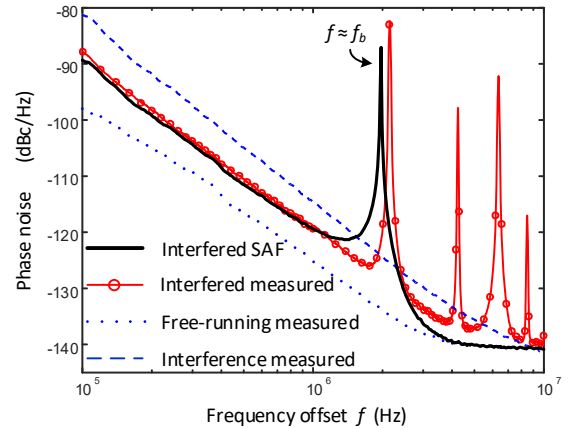


Fig. 4. Phase noise in the presence of an interferer with  $P_{in} = -29$  dBm and  $f_{in} = f_{osc} + 3$  MHz. The phase noise characteristic about  $f'_{osc}$  is pulled towards the interferer phase noise characteristic and noise resonances appear at  $kf_b$  frequency offsets.

Table I shows that, as expected from the theoretical analysis, the interfered oscillator measured phase noise is pulled towards that of the interferer as  $P_{in}$  increases. The measurements have been compared with the results of equation (25).

TABLE I  
PHASE NOISE @ 1 MHz VERSUS INTERFERER POWER

$P_{in}$	Phase noise prediction (25)	Measured phase noise
-29 dBm	-119.7 dBc/Hz	-119 dBc/Hz
-28 dBm	-115.45 dBc/Hz	-117 dBc/Hz
-24 dBm	-115 dBc/Hz	-115 dBc/Hz

#### IV. ANALYSIS OF THE EFFECT OF THE INTERFERER MODULATION

##### A. Phase modulation

In this Section, the influence of a phase-modulated (PM) interferer on the free-running oscillation will be analyzed. The modulation signal is modeled by the input source time-varying phase  $\psi(t)$ , considered as a stochastic process, whereas the amplitude component  $I_g$  is fixed to a constant value. As a difference from the previous phase noise analysis, in this case the magnitude of  $\psi(t)$  is not always small, and therefore linearization (18) is not applicable. In the presence of the interferer phase modulation, equation (4) becomes:

$$\begin{aligned} \dot{\phi} &= \Delta\omega + K_s \sin[\phi - \psi(t)] + K_c \cos[\phi - \psi(t)] \equiv \\ &\equiv g[\phi - \psi(t)] \end{aligned} \quad (26)$$

In order to study the modulation effect, the components corresponding to the noise sources have been removed from (26). In the following technique, these components can be included to analyze the noise-modulation combined effect, in a straightforward way.

In the case that the modulation signal  $\psi(t)$  contains frequency components of the order of  $f_b$ , equation (26) can be directly solved through time integration, as it has been done in [14] using a less elaborate SAF. Nevertheless, that method may become computationally demanding when the modulation signal  $\psi(t)$  is a narrow-band process with bandwidth  $\mathcal{B} \ll f_b$ . In such cases, the use of time-frequency methods is advisable

[21-23]. Here, the solution  $\phi(t)$  to equation (26) has been expressed considering that the process  $\psi(t)$  modulates the components  $\{f_b, \bar{P}\}$  in (13). These components are narrow band processes whose time variation is slow when compared with  $T_b = 1/f_b$ :

$$\phi(t) = \omega_b(t)t + \sum_{n=-N}^N P_n(t)e^{jn\omega_b(t)t} \quad (27)$$

with  $\omega_b(t) = 2\pi f_b(t)$ . Introducing expression (27) in equation (16), the spectrum in the presence of a PM interferer is obtained:

$$X_1(t) \approx V_1 e^{j\phi(t)} = \sum_{k=-M}^M X_1^k(t) e^{jk\omega_{b0}t} \quad (28)$$

with  $\omega_{b0}$  being the beat frequency in absence of modulation ( $\psi = 0$ ). The harmonic components  $X_1^k(t)$  become time varying due to the effect of the modulation signal. In particular, as stated in the previous Section, the PM spectrum about the oscillation frequency  $f'_{osc} \equiv f_1$  is given by the term  $X_1^1(t)$ . To obtain this term, in the first place, a quasi-static analysis of the effect of the narrow-band PM interferer on the phase shift  $\phi(t)$  will be carried out. Using this analysis, the expression of  $X_1^1(t)$  in terms of the time-varying components  $\{f_b(t), \bar{P}(t)\}$  will be obtained. Finally, a technique to simulate these components will be derived.

### 1) Quasi-static approach

To illustrate the effect of the PM interferer on the oscillation component  $X_1^1(t)$ , the case of a step phase modulation signal has been considered. In this case, the process  $\psi(t)$  is given by the deterministic signal:

$$\psi(t) = \begin{cases} 0, & t < t_s \\ \psi_1, & t \geq t_s \end{cases} \quad (29)$$

To clarify the effect of the step modulation, the evolution of the system trajectory in the phase-space  $(\phi, \dot{\phi})$  has been shown in Fig. 5(a). For  $t < t_s$ , the trajectory lies on the curve  $(\phi, g(\phi))$ , and the time domain expression for the phase variable is given by equation (13):

$$\phi(t) \equiv \phi_0(t) = \omega_{b0}t + P_0 + \sum_{n \neq 0} P_n e^{jn\omega_{b0}t}, \quad t < t_s \quad (30)$$

At  $t = t_s$  the trajectory jumps to the curve  $(\phi, g(\phi - \psi_1))$ . The time domain expression for the phase variable beyond this point is:

$$\begin{aligned} \dot{\phi} &= g(\phi - \psi_1) \rightarrow \phi(t) \equiv \phi_1(t) = \phi_0(t + \tau) + \psi_1 = \\ &= \omega_{b0}t + P_0(\tau) + \psi_1 + \sum_{n \neq 0} P_n(\tau) e^{jn\omega_{b0}t} \end{aligned} \quad (31)$$

where  $\tau$  is a constant time shift due to the system autonomy and with  $P_n(\tau)$  defined in (15). When compared to expression (30), equation (31) shows that the effect of the step PM is to shift the phase of the components  $P_n$  for  $n \neq 0$  and to make the amplitude of the dc component jump from  $P_0$  to  $P_0(\tau) + \psi_1$ . The order of magnitude of this jump can be bounded by applying the continuity property at  $t = t_s$ :

$$\begin{aligned} \phi_0(t_s) &= \phi_1(t_s) \rightarrow |\Delta P_0| = |P_0(\tau) + \psi_1 - P_0| = \\ &= \left| \sum_{n \neq 0} P_n e^{jn\omega_b t_s} (1 - e^{jn\omega_b \tau}) \right| \leq 2 \sum_{n \neq 0} |P_n| \end{aligned} \quad (32)$$

Equation (32) shows that the phase jump  $|\Delta P_0|$  due to an arbitrary modulation step is limited by the amplitude components  $|P_n|$ . The amplitude of the components  $P_n$  for  $n \neq 0$  is directly proportional to the interferer power. Therefore, in the case of a low power interferer,  $|\Delta P_0|$  will remain small for any arbitrary value  $\psi_1$  of the step PM. In the following, these results will be applied to obtain an expression of the modulated harmonic component  $X_1^1(t)$  at the oscillation frequency.

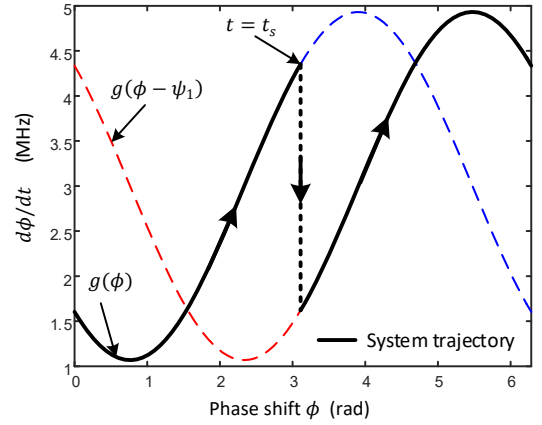


Fig. 5. Quasi-static approach. Effect of the step interferer on the evolution of the system trajectory in the phase-space.

### 2) Effect of the PM interferer at the oscillation frequency

The multi-tone spectrum in the vicinity of the oscillation frequency  $f'_{osc}$  is obtained as in (16) from the time varying harmonic component  $X_1(t)$  which, in the presence of a PM interferer, becomes:

$$\begin{aligned} X_1(t) &\approx V_1 e^{j\omega_b(t)t} \exp \left\{ \sum_{n=-N}^N jP_n(t) e^{jn\omega_b(t)t} \right\} = \\ &= V_1 e^{j[\omega_b(t)t + P_0(t)]} \exp \left\{ \sum_{n \neq 0} jP_n(t) e^{jn\omega_b(t)t} \right\} = \\ &= V_1 e^{j[\omega_b(t)t + P_0(t)]} + O(\alpha), \quad \alpha = \sum_{n \neq 0} jP_n(t) e^{jn\omega_b(t)t} \end{aligned} \quad (33)$$

where expression (27) for the phase shift  $\phi(t)$  has been applied. In equation (33), the signal  $X_1(t)$  is generated by the addition of two terms. Comparing this result with equation (28) it is seen that the first term  $V_1 e^{j[\omega_b(t)t + P_0(t)]}$  is contributes entirely to  $X_1^1(t)$ . The second term  $O(\alpha)$  produces PM harmonic components at  $f_k$ , for  $k = -M, \dots, M$ . Derivation (29)-(31) showed that the amplitudes of the components  $P_n$  for  $n \neq 0$  remain small for a narrow band low power PM interferer. Then, the contribution of  $O(\alpha)$  to the term  $X_1^1(t)$  can be neglected, obtaining:

$$X_1^1(t) \approx V_1 e^{j\phi(t)}, \quad \phi(t) = [\omega_b(t) - \omega_{b0}]t + P_0(t) \quad (34)$$

Approximation (34) shows that the PM interferer modulates the phase  $\varphi(t)$  of the harmonic component  $X_1^1$  at the oscillation frequency  $f'_{osc}$ . Note that, in the previous quasi-state analysis, the effect of a step phase modulation of arbitrary magnitude  $\psi_1$  on the oscillation phase is:

$$\Delta\varphi = P_0(\tau) + \psi_1 - P_0 = \Delta P_0 \quad (35)$$

where  $|\Delta P_0|$  is limited by the small amplitude components  $|P_n|$ , as described in (32). Considering this case as a quasi-static approximation of a narrow band PM interferer, result (35) suggests that such modulation will produce a small perturbation on the phase  $\varphi(t)$ . In order to verify this effect, in the following, a technique to simulate the time-varying phase  $\varphi(t)$  in the presence of the PM interferer will be derived.

### 3) Time-frequency simulation technique

In the first place, the function  $\phi(t)$  in the presence of a narrow band PM interferer is expressed in terms of a bi-variate function:

$$\begin{aligned} \phi(t) &= \hat{\phi}(t, t), \\ \hat{\phi}(t_1, t_2) &= \omega_b(t_1)t_2 + \sum_{n=-N}^N P_n(t_1)e^{jn\omega_b(t_1)t_2} \end{aligned} \quad (36)$$

with  $\omega_b(t_1) = 2\pi f_b(t_1) = 2\pi/T_b(t_1)$  and the time variables  $t_1$  and  $t_2$  representing the slow and fast scales, respectively. Applying the same procedure to the nonlinear function  $g[\phi - \psi(t)]$  in (26) we obtain:

$$\begin{aligned} g[\phi - \psi(t)] &= g(t) = \hat{g}(t, t), \\ \hat{g}(t_1, t_2) &= \Delta\omega + K_s \sin[\hat{\phi}(t_1, t_2) - \psi(t_1)] + \\ &\quad + K_c \cos[\hat{\phi}(t_1, t_2) - \psi(t_1)] \end{aligned} \quad (37)$$

In [7, 22] the method to obtain the equation governing the bi-variate process  $\hat{\phi}(t_1, t_2)$  associated with a generic ordinary differential equation (ODE) is derived. When applying this derivation to equation (26), the following Partial Differential equation (PDE) is obtained:

$$\left. \frac{\partial \hat{\phi}(t_1, t_2)}{\partial t_1} \right|_{t_1=t_2} + \left. \frac{\partial \hat{\phi}(t_1, t_2)}{\partial t_2} \right|_{t_1=t_2} = \hat{g}(t_1, t_2)|_{t_1=t_2} \quad (38)$$

In order to get the equation associated to the slow time scale  $t_1$ , function  $\hat{g}(t_1, t_2)$  is expressed as:

$$\hat{g}(t_1, t_2) = \sum_{n=-N}^N G_n(t_1)e^{jn\omega_b(t_1)t_2} \quad (39)$$

Now, introducing expressions (36), (37) and (39) in (38) and equating the terms that correspond to the same harmonic order the following system of first-order ODEs is obtained:

$$[\omega_b(t_1) + \dot{\omega}_b(t_1)t_1][jnP_n(t_1) + \delta_n^0] + \dot{P}_n(t_1) = G_n(t_1) \quad (40)$$

with  $n = -N, \dots, N$ . The set  $\{f_b, \bar{P}\}$  containing  $2N + 2$  components is the set of state variables of system (40). In accordance with analysis (15), the additional equation  $P_1^i = 0$  is included to balance the number of equations and variables. System (40) can be solved through Backward-Euler time-

integration. Using this technique, the ODEs in (40) are discretized at each time value  $t_1$ , providing an algebraic system of the form:

$$H_n[f_b(t_1), \bar{P}_n(t_1)] = G_n(t_1), \quad n = -N, \dots, N \quad (41)$$

where the unknowns  $f_b(t_1), \bar{P}_n(t_1)$  must be solved for each  $t_1$ . The components  $G_n(t_1)$  are calculated in three steps:

- The function  $\hat{\phi}(t_1, t_2)$  is constructed from  $\{f_b(t_1), \bar{P}_n(t_1)\}$  as indicated in equation (36). The time variable  $t_2$  takes  $2N + 1$  equally spaced samples in the interval  $[0, T_b(t_1)]$ .
- The function  $\hat{g}(t_1, t_2)$  is constructed from  $\hat{\phi}(t_1, t_2)$  as in equation (37).
- The harmonic components  $G_n(t_1)$  are calculated as:

$$\{G_n(t_1)\}_{n=-N}^N = \mathcal{F}_{t_2}\{\hat{g}(t_1, t_2)\} \quad (42)$$

with the operator  $\mathcal{F}_{t_2}$  representing the Fast Fourier Transform (FFT) in the  $t_2$  variable. Once system (40) is solved, the set of state variables  $\{f_b(t), \bar{P}(t)\}$  is introduced in equation (35) to obtain the slow varying phase  $\varphi(t)$  providing the phase modulation at the oscillation frequency  $f'_{osc}$ . This technique has been applied to simulate the effect of a sinusoidal PM interferer with  $P_{in} = -25$  dBm,  $\Delta f = -3.6$  MHz. The modulation frequency and index are  $f_m = 100$  kHz and  $\Delta\psi_m = 0.3$  rad, respectively. In Fig. 6, the simulated and measured spectra of the PM interferer and the harmonic component  $X_1^1(t)$  have been compared. The resolution bandwidth and video bandwidth of the measured spectra is RBW = 10 kHz and VBW = 10 kHz (respectively).

As predicted by the quasi-static analysis, the sideband components about  $f'_{osc}$  due to the PM are highly attenuated with respect of those of the interferer. If these sidebands are too small, their observation in the measured spectrum can be tricky due to the noisy spectrum.

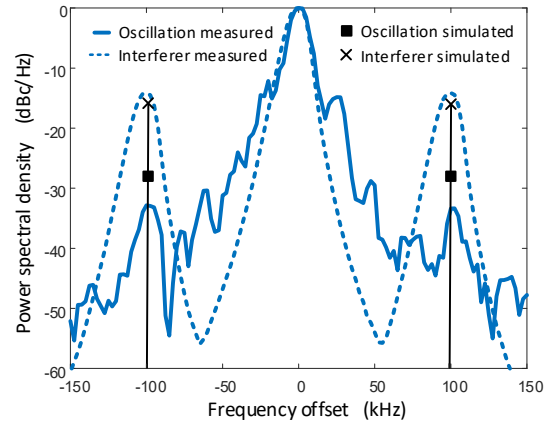


Fig. 6. Comparison between the simulated and measured spectra of the sinusoidal PM interferer and the harmonic component  $X_1^1(t)$ . An interferer with  $P_{in} = -25$  dBm,  $\Delta f = -3.6$  MHz has been introduced. The modulation frequency and index are  $f_m = 100$  kHz and  $\Delta\psi = 0.3$  rad, respectively

In the analysis of Fig. 6, the simulation technique predicts a 12 dB attenuation of the PM sidebands, whereas in the measurement 17 dB attenuation is observed. The discrepancy in the PM case is attributed to a combination of several facts.

The phase perturbation due to the phase-modulated interferer is simulated by integrating the envelope transient equation (40) in the slow time scale  $t_1$ . The oscillation is not phase-locked to the interferer. This means that system (26) is autonomous and therefore, for each time value, it remains invariant under a perturbation along a particular direction of the space  $(\phi, \dot{\phi})$ . As a consequence, the possible components of the numerical noise along this direction are accumulated, generating discrepancies. As observed in Fig. 8, these discrepancies are much smaller in the AM modulation case, where no numerical integration is required.

### B. Amplitude modulation

The case of an amplitude modulated (AM) interferer will be analyzed by expressing the equivalent current source  $i_g(t)$  as in (1), with the amplitude  $I_g(t)$  being a narrow-band process modeling the AM. Without loss of generality, in the absence of PM the interferer phase  $\psi(t)$  can be set to zero. As a result, equation (4) becomes:

$$\dot{\phi} = \Delta\omega + K_s(t) \sin \phi + K_c(t) \cos \phi \quad (43)$$

The phase shift  $\phi(t)$  can be expressed using structure (13) with the components  $\{f_b, \bar{P}\}$  being modulated by the interferer amplitude  $I_g(t)$ :

$$\phi(t) = \omega_b(t)t + \sum_{n=-N}^N P_n(t)e^{jn\omega_b(t)t} \quad (44)$$

$$\omega_b(t) = 2\pi f_b[I_g(t)], \quad P_n(t) = P_n[I_g(t)]$$

Assuming that the interferer amplitude  $I_g(t)$  remains small, approximation (33)-(34) is applicable to obtain the term  $X_1^1(t)$  providing the component at the oscillation frequency. Note that, as a difference from the case of the PM interferer, in this case the magnitude of the resulting phase modulation  $\varphi(t)$  at the oscillation frequency is not limited by condition (32). The time evolution of the phase shift  $\phi(t)$  can be simulated for a realization of  $I_g(t)$  using the technique described in Section IV.A.3 and then calculate the term  $X_1^1(t)$  from equation (34) to obtain the spectrum  $X_1^1(f)$  about the oscillation frequency  $f'_{osc}$ .

Deeper insight on the effect of the AM interferer can be gained by taking into account that, in the case of a narrow-band AM interferer, the phase modulation  $\varphi(t)$  in (34) produces a spurious frequency modulation (FM) of the oscillation component that can be approximated by:

$$\begin{aligned} \dot{\phi}(t) &\approx \omega_b[I_g(t)] - \omega_{b0} \rightarrow \\ &\rightarrow \varphi(t) \approx \int_0^t \omega_b[I_g(s)]ds - \omega_{b0}t \end{aligned} \quad (45)$$

with  $\omega_{b0}$  being the beat frequency value for a given arbitrary value  $I_{g0}$  of the interferer amplitude. In (45) the contribution of the terms  $\dot{\omega}_b(t)$  and  $\dot{P}_0(t)$  to  $\dot{\phi}(t)$  have been neglected. This is because, due to the system autonomy, the beat frequency  $f_b[I_g(t)]$  may vary freely with the interferer amplitude whereas  $\omega_b(t)$  and  $P_0(t)$  are slow-varying signals whose time derivatives are comparatively small. The function  $f_b(I_g)$  can be easily calculated with the frequency domain technique

described in Section III. This function has been represented Fig. 7 for the case of an interferer with  $\Delta f = -3.6$  MHz. For the analysis, system (14) has been solved with  $N = 5$  harmonics.

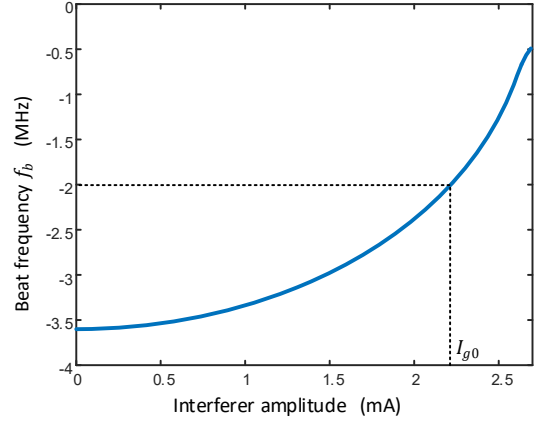


Fig. 7. Variation of the beat frequency  $f_b(I_g)$  for an interferer at  $f_{in} = f_{osc} + 3.6$  MHz.

In order to compare the effect of AM and PM interferers, the function  $f_b(I_g)$  of Fig. 7 has been used to analyze the FM produced at the oscillation frequency by a sinusoidal AM interferer of the form:

$$I_g(t) = I_{g0} + \Delta I_g \sin 2\pi f_m t \quad (46)$$

where  $I_{g0}$  produces an interferer power  $P_{in} = -25$  dBm,  $f_m = 100$  kHz and  $\Delta I_g$  has been set to produce the same modulation power spectrum about  $f'_{osc}$  as in the previous PM example of Fig. 6. Introducing the signal (46) into expression (45), the sidebands of the FM component  $X_1^1(t) \approx V_1 e^{j\varphi(t)}$  at  $f_m$  have been obtained, with the result of Fig. 8. The resolution bandwidth and video bandwidth of the measured spectra is RBW = 10 kHz and VBW = 10 kHz (respectively). The mean amplitude value  $I_{g0}$  has been marked in Fig. 7. Comparing Fig. 6 and 7, it is observed that the relative sidebands of the AM interferer are much lower than in the PM case and produce a similar spurious modulation at the oscillation component. This indicates that, in this case, the oscillation phase is more sensitive to the AM interferer than to the PM one due to the free variation of the beat frequency with the interferer amplitude. Note that the discrepancies between simulation and measurements appearing in Fig. 6 are much smaller in the AM modulation case, where no numerical integration is required.

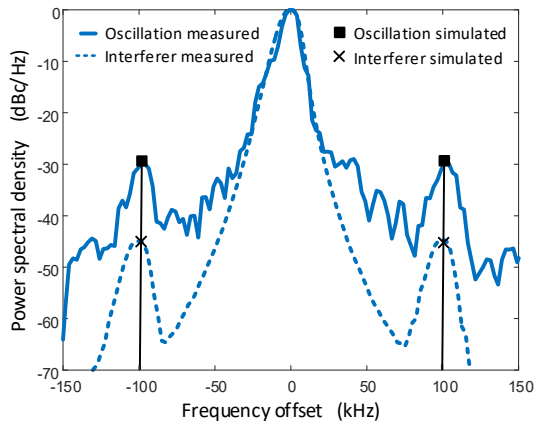


Fig. 8. Comparison between the simulated and measured spectra of the sinusoidal AM interferer and the harmonic component  $X_1^1(t)$ . An interferer with  $P_{in} = -25$  dBm,  $\Delta f = -3.6$  MHz has been introduced. The modulation frequency and index are  $f_m = 100$  kHz and  $\Delta I_g/I_{g0} = 1\%$ , respectively

Finally, in Fig. 9 the measured phase noise spectrum in the presence of a sinusoidal PM interferer with  $P_{in} = -25$  dBm,  $\Delta f = -3.6$  MHz has been introduced. The modulation frequency and index are  $f_m = 1$  MHz and  $\Delta\psi = 1$  rad, respectively. As predicted by the theoretical analyses of Sections III-IV, the components of the PM interferer perturb the phase noise spectrum in the vicinity of the frequency offsets  $f_m$  and  $|f_{osc} - f_{in}|$ . For comparison, the phase noise simulation using equation (25) has been superimposed. If the PM modulation index is low enough, superposition principle applies and the PSD of the phase perturbation resulting from simulation (41) can be added to the phase noise PSD, considering that both processes are uncorrelated. The spurious PM components are better observed in the spectrum analyzer than in the phase-noise characteristic. For this reason, we consider more accurate to compare the simulated PM effect with the signal power spectrum, as in Fig. 6.

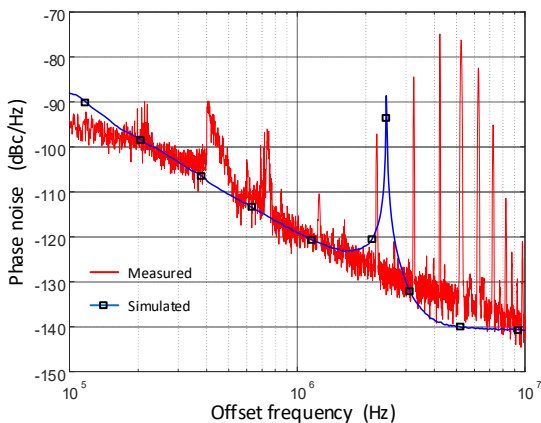


Fig. 9. Phase noise spectrum in the presence of a sinusoidal PM interferer with  $P_{in} = -25$  dBm,  $\Delta f = -3.6$  MHz. The modulation frequency and index are  $f_m = 1$  MHz and  $\Delta\psi = 1$  rad, respectively

## V. CONCLUSION

The influence of the interferer phase noise and modulation

on the free-running oscillator spectrum has been analyzed. A semi-analytical formulation has been derived for the oscillation phase noise. This leads to a simple and insightful equation describing the pulling effect of the interfered oscillator phase noise towards that of the interference signal. The cases of PM and AM interferers have been studied, providing efficient simulation techniques to predict their effects on the oscillation spectrum. The mechanisms producing spurious modulation of the oscillator phase have been explained in detail. All the predictions have been verified by measurements in a FET-based oscillator at 2.5 GHz.

## REFERENCES

- [1] B. Razavi, "A study of injection locking and pulling in oscillators," *IEEE J Solid State Circuits*, vol. 39, pp. 1415-1424, 2004.
- [2] S. Yen and T. Chu, "An nth-harmonic oscillator using an N-push coupled oscillator array with voltage-clamping circuits," 2003, pp. 2169-2172.
- [3] Z. Li and K. Wu, "On the leakage of FMCW radar front-end receiver," *2008 Global Symposium on Millimeter Waves*, 2008, pp. 127-130.
- [4] S. Sancho, M. Ponton, A. Suarez and F. Ramirez, "Analysis of Injection Pulling in Phase-Locked Loops With a New Modeling Technique," *IEEE Transactions on Microwave Theory and Techniques*, vol. 61, pp. 1200-1214, 2013.
- [5] S. Sancho, M. Ponton and A. Suarez, "Nonlinear technique for the analysis of the free-running oscillator phase noise in presence of an interference signal," *International Microwave Symposium*, Honolulu, 2017.
- [6] U. L. Rohde, *Microwave and Wireless Synthesizers: Theory and Design*. Wiley-Interscience, 1997.
- [7] A. Mehrotra and A. Sangiovanni-Vincentelli, *Noise Analysis of Radio-Frequency Circuits*. Kluwer Academic Publisher (Springer), 2004.
- [8] F. K. Wang, T. S. Hornig, K. C. Peng, J. K. Jau, J. Y. Li and C. C. Chen, "Single-Antenna Doppler Radars Using Self and Mutual Injection Locking for Vital Sign Detection With Random Body Movement Cancellation," *IEEE Transactions on Microwave Theory and Techniques*, vol. 59, pp. 3577-3587, 2011.
- [9] K. Siddiq, R. J. Watson, S. R. Pennock, P. Avery, R. Poulton and B. Dakin-Norris, "Phase noise analysis in FMCW radar systems," *2015 European Radar Conference (EuRAD)*, 2015, pp. 501-504.
- [10] T. S. Parker and L. O. Chua, *Practical Numerical Algorithms for Chaotic Systems*. Berlin ; New York: Springer Verlag, 1989.
- [11] V. Rizzoli, F. Matri and D. Masotti, "General noise analysis of nonlinear microwave circuits by the piecewise harmonic balance technique," *IEEE Trans. Microwave Theory Tech.*, vol. 42, pp. 807-819, 1994.
- [12] A. Suarez and S. Sancho, "Application of the envelope-transient method to the analysis and design of autonomous circuits," *International Journal of RF and Microwave Computer-Aided Engineering*, vol. 15, pp. 523-535, 2005.
- [13] A. Suarez, *Analysis and Design of Autonomous Microwave Circuits*. Wiley, 2009.
- [14] J. Dominguez, A. Suarez and S. Sancho, "Semi-analytical formulation for the analysis and reduction of injection-pulling in front-end oscillators," *Microwave Symposium Digest, 2009. MTT '09. IEEE MTT-S International*, 2009, pp. 1589-1592.
- [15] S. Sancho, F. Ramirez and A. Suárez, "Stochastic Analysis of Cycle Slips in Injection-Locked Oscillators and Analog Frequency Dividers," *IEEE Transactions on Microwave Theory and Techniques*, vol. 62, pp. 3318-3332, 2014.
- [16] F. Ramirez, M. Ponton, S. Sancho and A. Suarez, "Phase noise of injection-locked oscillators and frequency dividers," *IEEE Transactions on Microwave Theory and Techniques*, vol. 56, pp. 393-407, Feb. 2008.
- [17] F. X. Kaertner, "Analysis of white and  $f^{alpha}$  noise in oscillators," *Int. Journal of Circuit Theory and Applications*, vol. 18, pp. 485-519, 1990.
- [18] A. Demir, "Phase noise and Timig Jitter in oscillators with colored noise sources," *IEEE Transactions on Circuits and Systems-I: Fundamental Theory and Applications*, vol. 49, pp. 1782-1791, December. 2002.
- [19] R. Quéré, E. Ngoya, M. Camiade, A. Suarez, M. Hessane and J. Obregon, "Large signal design of broadband monolithic microwave frequency dividers and phase-locked oscillators," *IEEE Trans. Microwave Theory Tech.*, vol. 41, pp. 1928-1938, November., 1993.
- [20] A. Suarez and R. Quéré, *Stability Analysis of Nonlinear Microwave Circuits*. Boston: Artech-House, 2003.
- [21] E. Ngoya and R. Larcheveque, "Envelope transient analysis: A new

method for the transient and steady-state analysis of microwave communication circuits and systems," *IEEE Microwave Theory and Techniques Symposium*, June. 1996.

[22] H. G. Brachtendorf, G. Welsch, R. Laur and A. Bunse-Gerstner, "Numerical steady state analysis of electronic circuits driven by multi-tone signals," *Electrical Engineering*, vol. 79, pp. 103-112, 1996.

[23] J. C. Pedro and N. B. Carvalho, "Simulation of RF circuits driven by modulated signals without bandwidth constraints," 2002, pp. 2173-2176.

[24] M. Ponton, E. Fernandez, A. Suarez and F. Ramirez, "Optimized Design of Pulsed Waveform Oscillators and Frequency Dividers," *IEEE Transactions on Microwave Theory and Techniques*, vol. 59, pp. 3428-3440, 2011.

[25] S. Sancho, A. Suarez, J. Dominguez and F. Ramirez, "Analysis of Near-Carrier Phase-Noise Spectrum in Free-Running Oscillators in the Presence of White and Colored Noise Sources," *IEEE Transactions on Microwave Theory and Techniques*, vol. 58, pp. 587-601, 2010.

[26] J. A. Mullen and D. Middleton, "Limiting forms of the FM spectra," *Proceedings of the I.R.E.*, vol. 45, pp. 874-877, Jun. 1957.

[27] S. Sancho, A. Suarez and F. Ramirez, "General Phase-Noise Analysis From the Variance of the Phase Deviation," *IEEE Transactions on Microwave Theory and Techniques*, vol. 61, pp. 472-481, 2013.

[28] A. Suarez, S. Sancho, S. Ver Hoeye and J. Portilla, "Analytical comparison between time- and frequency-domain techniques for phase-noise analysis," *IEEE Transactions on Microwave Theory and Techniques*, vol. 50, pp. 2353-2361, 2002.



**Sergio Sancho** (A'04–M'04) received the degree in Physics from Basque Country University in 1997. In 1998 he joined the Communications Engineering Department of the University of Cantabria, Spain, where he received the Ph.D. degree in Electronic Engineering in February 2002. At present, he works at the University of Cantabria, as an Associate Professor of its Communications Engineering

Department. His research interests include the nonlinear analysis of microwave autonomous circuits and frequency synthesizers, including stochastic and phase-noise analysis.



**Mabel Pontón** (S'08–M'11) was born in Santander, Spain. She received the bachelor's degree in telecommunication engineering, master's degree in information technologies and wireless communications systems, and Ph.D. degree from the University of Cantabria, Santander, in 2004, 2008, and 2010, respectively.

In 2006, she joined the Communications Engineering Department, University of Cantabria.

From 2011 to 2013, she was with the Group of Electronic Design and Applications, Georgia Institute of Technology, Atlanta, GA, USA, as a Post-Doctoral Research Fellow.

Her current research interests include the nonlinear analysis and simulation of radiofrequency and microwave circuits, with an emphasis on phase-noise, stability, and bifurcation analysis of complex oscillator topologies.



**Almudena Suárez** (M'96–SM'01–F'12) was born in Santander, Spain. She received the Electronic Physics and Ph.D. degrees from the University of Cantabria, Santander, Spain, in 1987 and 1992, respectively, and the Ph.D. degree in electronics from the University of Limoges, Limoges, France, in 1993. She is currently a Full Professor with the Communications Engineering Department, University of Cantabria. She co-authored *Stability*

*Analysis of Nonlinear Microwave Circuits* (Artech House, 2003) and authored *Analysis and Design of Autonomous Microwave Circuits* (IEEE-Wiley, 2009). Prof. Suárez is a member of the Technical Committees of the IEEE International Microwave Symposium (IMS), the European Microwave Conference. She was an IEEE Distinguished Microwave Lecturer from 2006 to 2008, with the talk "Stability analysis and stabilization of power amplifiers." She is the editor-in-chief of *International Journal of Microwave and Wireless Technologies*, from Cambridge Journals. She is an associate editor of IEEE Microwave Magazine. She is a member of the "Board of Directors" of the European Microwave Association. She was the coordinator of the Communications and Electronic Technology Area for the Spanish National Evaluation and Foresight Agency (ANEP) between 2009 and 2013.